

Changes in non-oscillatory features of the cortical sensorimotor rhythm in Parkinson's disease across age

Authors

Mikkel C. Vinding* 1), Allison Eriksson 1)2), Cassia Man Ting Low 1)3), Josefine Waldthaler 4)5), Daniel Ferreira 6,7), Martin Ingvar 1), Per Svenningsson 4), Daniel Lundqvist 1).

Affiliations

1. NatMEG, Department of Clinical Neuroscience, Karolinska Institutet, Sweden.
2. Department of Women's and Children's Health, Uppsala University, Sweden.
3. Cognitive Neuroimaging Centre, Lee Kong Chien School of Medicine, Nanyang Technological University, Singapore.
4. Section of Neurology, Department of Clinical Neuroscience, Karolinska Institutet, Sweden.
5. Department of Neurology, University Hospital Marburg, Marburg, Germany.
6. Division of Clinical Geriatrics, Center for Alzheimer's Research, Department of Neurobiology, Care Sciences, and Society, Karolinska Institutet, Stockholm, Sweden.
7. Department of Radiology, Mayo Clinic, Rochester, MN, USA.

Corresponding author

Mikkel C. Vinding

Department of Clinical Neuroscience

Karolinska Institutet

Nobels väg 9, D2

171 77 Stockholm

Sweden

Email: mikkel.vinding@ki.se

1 Abstract

2 Parkinson's disease (PD) is associated with changes in neural activity in the sensorimotor alpha and
3 beta bands. Using magnetoencephalography (MEG), we investigated the role of spontaneous neuronal
4 activity within the somatosensory cortex in a large cohort of early- to mid-stage PD patients (N = 78)
5 and age- and sex matched healthy controls (N = 60) using source reconstructed resting-state MEG. We
6 quantified features of the time series data in terms of oscillatory alpha power, beta power, and 1/f
7 broadband characteristics using power spectral density, and also characterised transient beta burst
8 events in the time-domain signals. We examined the relationship between these signal features and the
9 patients' disease state, symptom severity, age, sex, and cortical thickness.

10 PD patients and healthy controls differed on PSD broadband characteristics, with PD patients showing
11 a steeper 1/f exponential slope and higher 1/f offset. PD patients further showed a steeper age-related
12 decrease in the burst rate. Out of all the signal features of the sensorimotor activity, only burst rate was
13 associated with increased severity of bradykinesia. Our study shows that general non-oscillatory
14 features (broadband PSD slope and offset) of the sensorimotor signals are related to disease state and
15 *oscillatory burst rate* scales with symptom severity in PD.

16 1 Introduction

17 Parkinson's disease (PD) is a common neurodegenerative disease characterised by a gradual
18 accumulation of Lewy bodies and death of dopaminergic neurons.^{1,2} The Lewy body pathology of PD
19 begins long before the manifestation of motor symptoms. Accumulation of Lewy bodies is initially
20 found in the olfactory bulb and brain stem and then spreads to the substantia nigra pars compacta,
21 followed by several brain regions, including the basal ganglia and the neocortex.³ The progressive
22 structural and neurochemical changes in PD are accompanied by widespread functional changes in
23 neuronal activity, which in turn lead to worsening clinical signs and symptoms such as tremor, rigidity,
24 and bradykinesia and co-occurring non-motor symptoms like sleep disorders, depression, fatigue, and
25 cognitive deficits.¹

26 The changes in brain function in PD are particularly prominent in the oscillatory activity of neurons.⁴
27 In PD, spontaneous oscillatory beta band (13–30 Hz) activity in the sub-thalamic nucleus (STN)
28 exhibits a systematic disease-related increase in synchronicity that is related to the dopamine level^{5–8},
29 and correlates with the severity of bradykinesia and rigidity symptoms.^{9,10} Changes in the beta band
30 extend beyond the STN through the basal ganglia-thalamic cortical sensorimotor network. The cortical
31 manifestation of the disease-related changes in the sensorimotor network can be measured non-
32 invasively from the cortex, using electro- or magnetoencephalography (EEG/MEG). Such non-invasive
33 neural recordings can potentially provide easily available prospective biomarkers of disease or
34 symptom-related neural changes in PD. Increased oscillatory beta-band activity in the sensorimotor
35 cortex has been linked to increased symptom severity, such as rigidity and bradykinesia.^{11,12} The role of
36 dopamine on the cortical beta band is, however, still unclear. There is no consensus on how
37 dopaminergic medication affects cortical beta-band power, with some studies reporting no effects^{11,13–}

38 ¹⁵ and others an increase in beta-band power.¹⁶⁻¹⁸ Deep brain stimulation of the STN in PD patients has
39 been shown to lead to a decrease in the power of spontaneous activity in the cortical sensorimotor beta
40 and alpha (8-12Hz) bands^{19,20} (but see also^{16,21}).

41 Importantly, there is evidence that the beta-band changes are not in the same direction across the
42 different stages of PD. For example, there are reports of increased cortical beta-band power in the early
43 stages of PD²², whereas the later stages are associated with decreased beta-band power.²³ Further, the
44 beta-band power is not the *only* feature of the sensorimotor rhythms that is altered in PD. Several
45 studies have found a shift in the beta-band centre frequency (the frequency at which the power
46 spectrum density peaks in the beta-band) towards a lower frequency in PD patients compared to
47 healthy controls.²⁴⁻²⁶ The shift towards lower beta-band centre frequency is more pronounced in PD
48 patients with dementia²⁷⁻³⁰ and correlates with reduced cognitive ability.^{26,31} Notably, the centre
49 frequency shift is detectable already in the early stages of PD²⁵ and does not seem to be affected by
50 dopaminergic medication.³² The changes in beta-band power and centre frequency in PD could indicate
51 that different features of the oscillatory beta-band activity reflect different underlying neural functions
52 expressed in the measured sensorimotor signals. Changes in beta-band power could be functionally
53 related to sensorimotor disturbances, and changes in centre frequency could be related to cognitive
54 function.

55 The characteristics of neuronal oscillatory activity may hold additional information of disease-related
56 changes in PD.³³ Both beta-band power and centre frequency reflect a quantification of power spectral
57 density (PSD). While these features can provide valuable information about disease-related changes in
58 PD, the PSD quantification of a neural time series provides a static summary of the oscillatory activity
59 across the entire time series. PSD does not account for inherent dynamics in this activity or changes in

60 the time series on shorter time scales—as is prevalent in neural time series. The beta-band exhibits a
61 great degree of variation over time and contains characteristic high-amplitude "bursts" that last about
62 50-200 ms, both in the cortical and sub-cortical beta-bands.^{34–37} Functionally, the transient bursts
63 appear to play a pivotal role in sensorimotor processing through the basal ganglia-thalamic-cortical
64 network. For instance, the presence of a beta burst in the sensorimotor cortex close to a tactile
65 stimulation decreased the likelihood of tactile detection³⁸, and the rate of beta bursts is shown to
66 decrease in the time leading up to a movement both in STN^{39–41} and in the sensorimotor cortex.^{42,43}

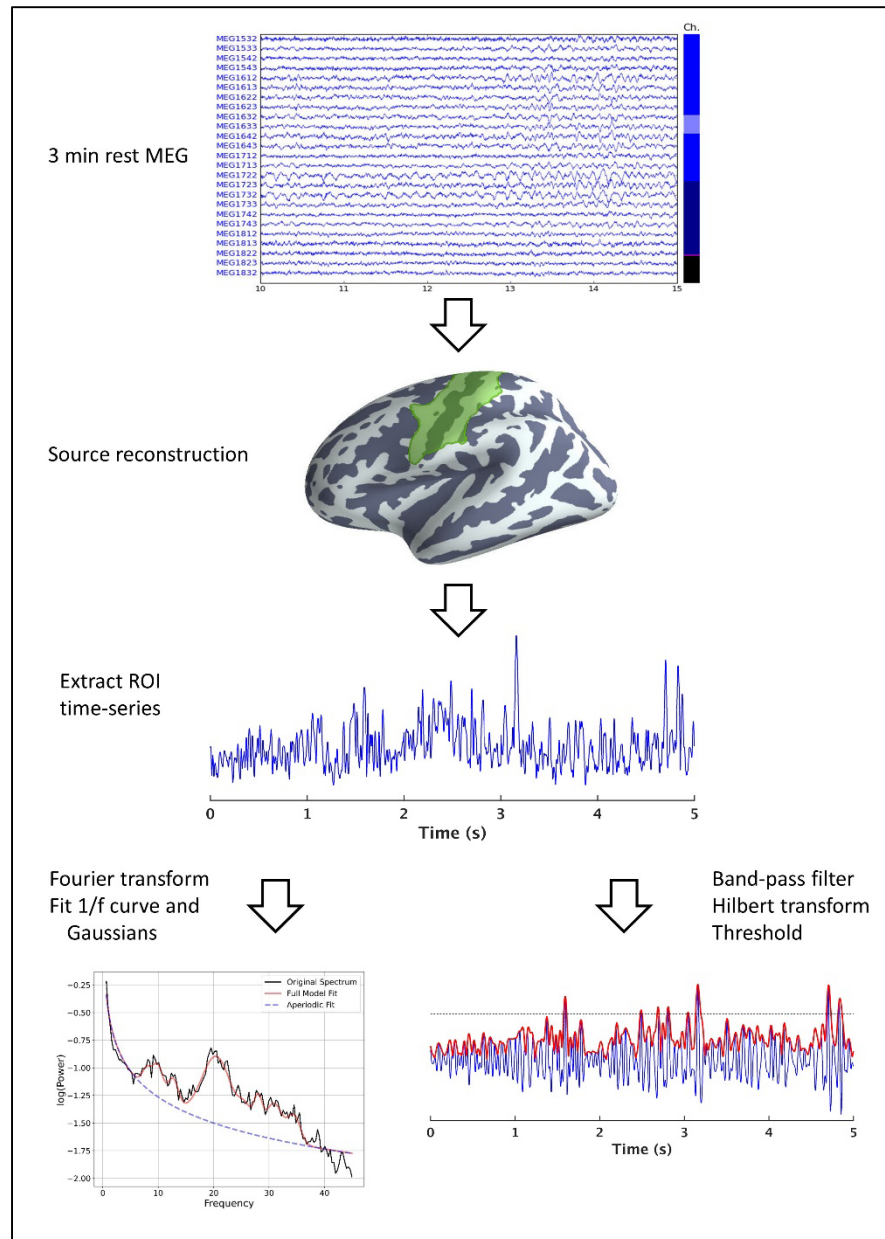
67 In PD, quantification of beta-band burst activity from recordings in the STN has shown that beta-burst
68 rate and duration are reduced by dopaminergic medication^{44,45} and deep brain stimulation.³⁷

69 Furthermore, PD patients exhibit a decrease in the rate of beta burst at the cortical level compared to
70 healthy controls.¹⁴ This decrease in beta burst rate is inversely related with increased severity of motor
71 symptoms;⁴⁶ particularly bradykinesia and postural-kinetic tremor symptoms, but there is not evidence
72 pointing to an effect of dopaminergic medication on cortical bursting properties.¹⁴ Notably, the burst
73 rate showed a higher sensitivity than PSD beta power for discriminating PD patients from healthy
74 controls, demonstrating that the choice of method for analysing beta-band features influences the
75 sensitivity of subsequent analyses. This is further complicated by the fact that in addition to disease-
76 related changes, these features likely differ with age,^{43,47} and the fact that most studies on oscillatory
77 changes in PD come from studies with small sizes.⁴⁸ The central challenge is quantifying the measured
78 neural signals to extract the disease's relevant features from the signals, be it the spectral power, centre
79 frequencies, or burst-like features.

80 In the current study, we aimed to compare how different oscillatory features of cortical sensorimotor
81 activity change in PD to elucidate what oscillatory features in the neural time-series differ between PD

82 patients and healthy controls and how these features are associated with different motor symptoms in
83 PD. We extracted the sensorimotor neural resting-state activity from source reconstructed resting-state
84 MEG signals in the sensorimotor cortex (Figure 1) and quantified the time-series in terms of the PSD in
85 the canonical mu-band (8-30 Hz).^{49,50} In addition to the band-specific analysis, we compared the 1/f
86 broadband characteristics of the PSD.^{51,52} Finally, we compared features of the sensorimotor rhythm in
87 terms of time-domain analysis of spontaneous transient bursts.^{14,38} We tested the hypotheses of altered
88 functional changes in PD by analysing how these features differed between PD patients and healthy
89 controls and further investigated the interactions with age and sex. As ageing is associated with
90 structural and functional changes in the sensorimotor cortex^{53,54}, we investigated if the potential
91 changes in sensorimotor activity in PD differed across age. Since both healthy ageing and PD disease
92 progression are linked to thinning of the cortex^{55,56}, we further included thickness of the sensorimotor
93 cortex in the analysis as a potential mediating factor on the sensorimotor activity that potentially also
94 interacts with disease state.

95 The central hypothesis was that there would be differences between healthy controls and PD in features
96 of the sensorimotor signals, but also that different features may be related to different functional
97 changes. We hypothesised that individual oscillatory features would reflect different underlying neural
98 functions in the sensorimotor system and thereby show different relationships to the clinical
99 manifestations of specific motor symptoms in PD. We tested this hypothesis in two steps: first,
100 examining the inter-relationship between all different measures, and subsequently, examining what
101 feature—or combination of features—best explained the variation in severity within each motor
102 symptom.



103

104 **Figure 1: Overview of the data processing pipeline.** Three minutes raw resting-state MEG data was
105 obtained from each participant. The signals were projected through a minimum-norm source
106 reconstruction to extract the activity in the sensorimotor cortex. We did a frequency decomposition of
107 the source reconstructed signal to calculate the PSD to which a 1/f and Gaussian curve were fitted to
108 extract the PSD features (Table 2). In addition, we quantified sensorimotor bursts in the signal time

109 series in the sensorimotor ROI by thresholding the envelope of the band-pass filtered (8-30 Hz) signal
110 to the mu-beta frequency range.

111 2 Results

112 To enable a sensitive assessment of disease-related oscillatory changes in PD, we aimed for a relatively
113 large cohort compared to other functional neuroimaging studies of PD patients (N=78) and healthy
114 controls (N=60), balanced across gender and age, and with gender- and age-matched groups (Table 1).

115 Table 1: Group-level summary of the participants included in the analysis. Mean (standard deviation).

Measure	Parkinson's patients	Healthy controls	Statistics
<i>N</i>	78	60	
<i>Sex (female/male)</i>	29/49	27/33	$\chi^2 = 0.57, p = 0.45$
<i>Age</i>	65.6 (9.5)	63.93 (8.4)	Welsh $t(138.0) = 1.08, p = 0.28$
<i>Disease duration</i>	4.4 (3.7) years	-	-
<i>LEDD</i>	548 (273) mg	-	-
<i>MDS-UPDRS-III</i>	18.9 (10.8)	-	-
<i>MoCA</i>	26.1 (2.8)	26.2 (2.1)	Welsh $t(136) = 0.10, p = 0.92$

116

117 Table 2: Summary explanations of the main outcome variables in the analysis

Variable category	Variable	Explanation
PSD	<i>Beta power</i>	The maximum peak in the 13-30 Hz band. Estimated as the height of the Gaussian function fitted to the PSD after regressing out the 1/f spectrum.

	<i>Beta centre frequency (Hz)</i>	The dominant frequency bin in the 13-30 Hz band. Estimated as the centre of the Gaussian function fitted to the 13-30 Hz range of the PSD after regressing out the 1/f spectrum.
	<i>Alpha power</i>	The maximum peak in the 8-12 Hz band. Estimated as the height of the Gaussian function fitted to the PSD after regressing out the 1/f spectrum.
	<i>Alpha centre frequency (Hz)</i>	The dominant frequency bin in the 8-12 Hz band. Estimated as the centre of the Gaussian function fitted to the 8-12 Hz range of the PSD after regressing out the 1/f spectrum.
	<i>1/f offset</i>	The intercept of the log-linear regression line estimated from the full PSD in the 0.5-40 Hz range.
	<i>1/f exponent</i>	The decay exponent ($1/f^k$) of the PSD, corresponding to the slope of the log-linear regression line, estimated from the full PSD in the 0.5-40 Hz range.
Burst	<i>Rate</i>	The number of burst events in the time series divided by the length of the time series
	<i>Duration (ms)</i>	The time point from where the signal envelope rise above the threshold until the next time point it drops below the threshold.
	<i>Interval (ms)</i>	The time point from where the signal envelope drops below the threshold until the next time point it rises above the threshold.
	<i>Amplitude</i>	The maximum envelope amplitude within a burst event.

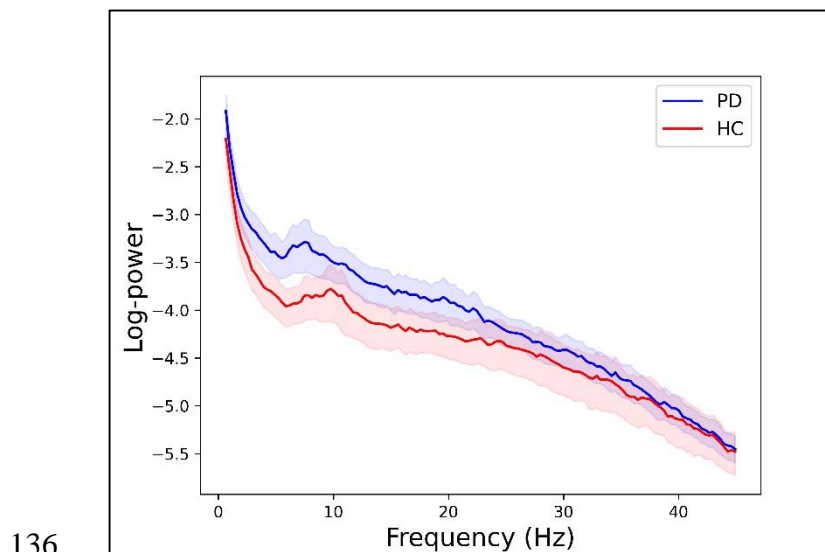
118

119 For the first analysis, we investigated how features in the resting-state activity from the sensorimotor
120 area quantified by features of the PSD and burst characteristics (see Table 2) differed as a function of
121 the predictors *group* (PD patients/healthy controls; Table 1), *age*, *sex*, and *cortical thickness* as well as
122 the interaction between the predictors.

123 2.1 PSD features

124 The PSD suggests an apparent group difference between PD patients and healthy controls in the alpha
125 and beta bands (Figure 2). However, analysing the oscillatory components of PSD by first adjusting for

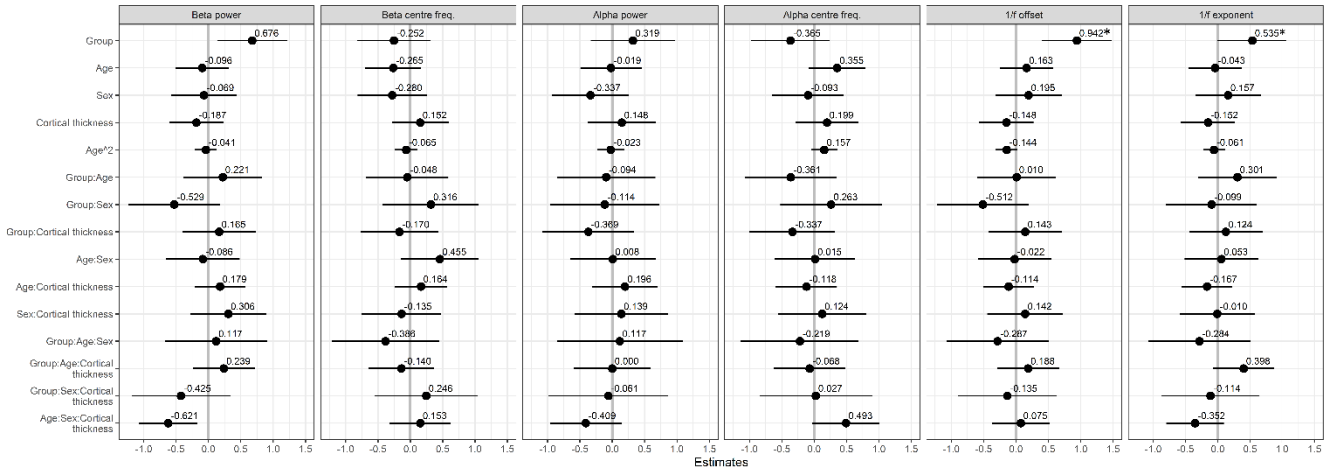
126 the broadband characteristic of the PSD⁵¹ removed the apparent group difference in the mu- and beta
127 band. Bayesian model comparison was used to test which predictors explained the variation in the PSD
128 (Bayes Factors (BF) > 3 taken as cutoff for substantial evidence for an effect of a given predictor⁵⁷).
129 The model comparison showed evidence for group differences on the 1/f offset (BF = 37.77) and 1/f
130 exponent (BF = 5.92). There were no substantial evidence of an effect beyond the threshold for
131 substantial evidence on any other PSD features. However, it might be worth noting that there was
132 anecdotal evidence of an effect of cortical thickness on 1/f exponent (BF = 1.73), an interaction effect
133 between age and group on alpha centre frequency (BF = 1.43), and only minute evidence for a group
134 difference on beta power (BF = 1.28). The coefficients of regression models analysing the effect of the
135 predictors on PSD for all outcome measures are presented in Figure 3.



137 **Figure 2: Group-level PSD.** Grand average PSD (mean+standard error) for the PD group (blue) and
138 healthy control group (red).

139 Analysing the PSD by regressing out the 1/f contribution to the spectrum, the difference between PD
140 patients and healthy controls is not so much in the canonical beta- and alpha bands but manifests in the

141 broadband characteristics of the signal. The 1/f intercept was 23.5% [CI: 11.8:33.7%] higher for PD
 142 patients than healthy controls, and PD patients had on average 11.9% [CI: -30.4:3.8%] steeper 1/f
 143 exponential slope compared to healthy controls.



144

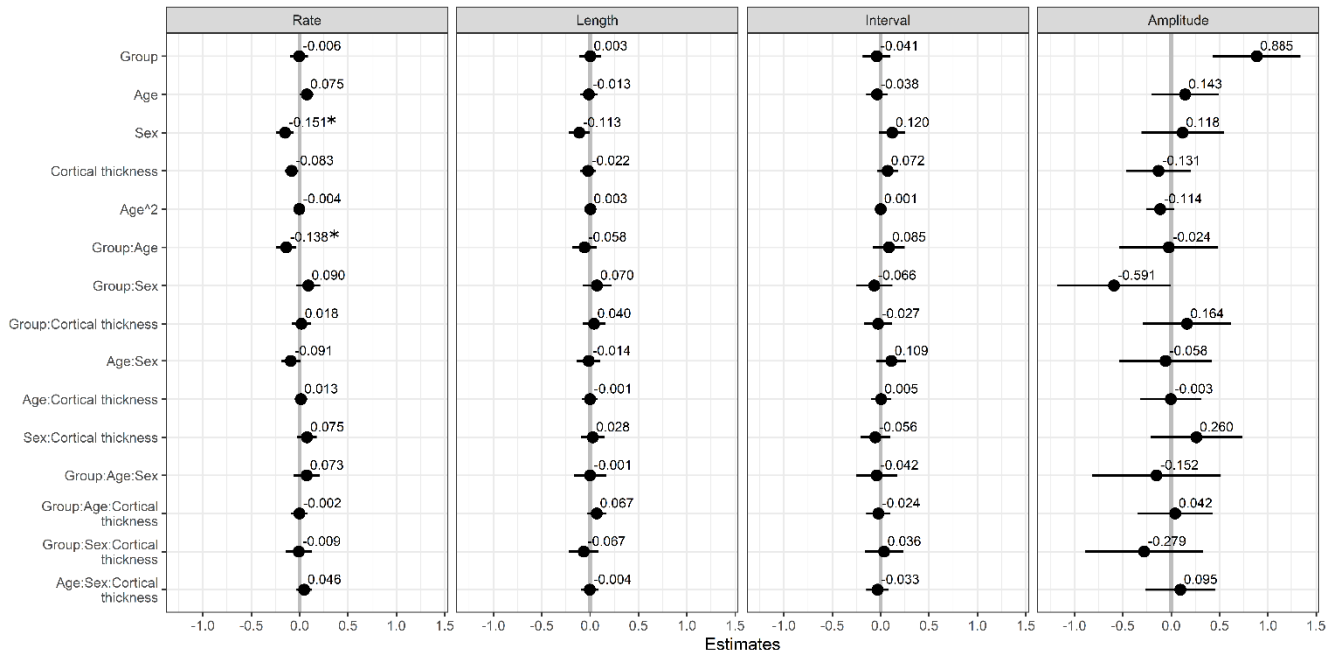
145 **Figure 3: Regression analysis of PSD features.** Standardized regression coefficients for the analyses
 146 of sensorimotor PSD features as a function of group, age, sex, cortical thickness and the interaction
 147 between these factors. * indicate factors with Bayes Factor > 3 in the model comparison.

148 **2.2 Burst features**

149 The view of sensorimotor oscillatory activity has recently changed from a steady oscillating signal to
 150 viewing the activity in the sensorimotor bands occurring in short bursts. We compared features of the
 151 sensorimotor rhythm in terms of time-domain analysis of spontaneous transient bursts in the time
 152 series. Model comparison to test which predictors explained the variation in the burst features gave
 153 evidence for an interaction effect between group and age on the burst rate (BF = 33.57) and a main
 154 effect of sex on the burst rate (BF = 4.34). Model coefficients are displayed in Figure 4.

155 The age-related effects from the model amount to a change in burst rate of -0.7% [CI: -1.6:0.2] per year
 156 for female PD patients and -1.7% [CI: -3.1:-0.3] change in burst rate per year for male PD patients,

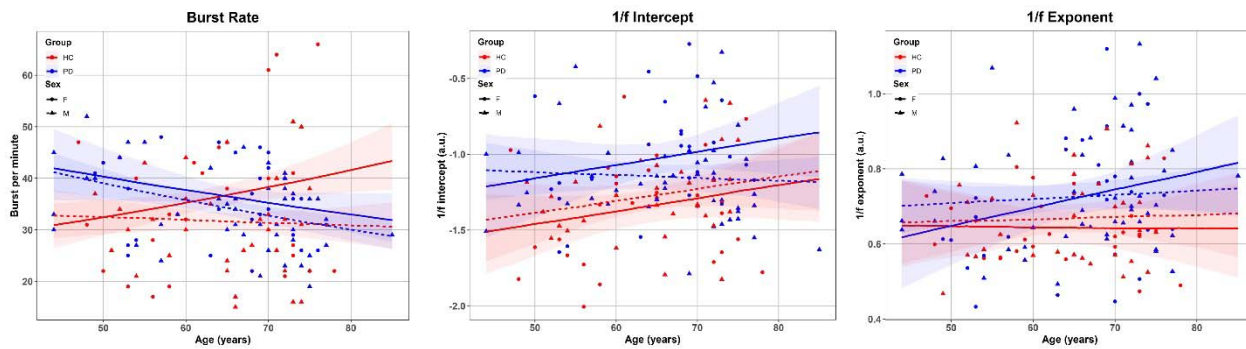
157 whereas female controls had a relative increase in burst rate of 0.8% [CI: 0.1:1.7] per year and male
 158 controls had a stable trend of -0.2% [CI: -1.0:0.6] change per year.



159

160 **Figure 4: Regression analysis of burst features.** Standardized regression coefficients for the analyses
 161 of burst features as a function of group, age, sex, cortical thickness and the interaction between these
 162 factors. * indicate factors with Bayes Factor > 3 in the model comparison.

163 No other predictors showed evidence of an effect beyond the threshold for substantial evidence on
 164 neither burst length, the interval between bursts, nor burst amplitude. There was anecdotal evidence
 165 (i.e. $1/3 < BF < 3$) for a group difference in burst amplitude ($BF = 2.08$) as well as an interaction effect
 166 of age and cortical thickness on the burst rate ($BF = 1.43$), and an interaction between sex and cortical
 167 thickness on the burst rate ($BF = 1.86$).



168

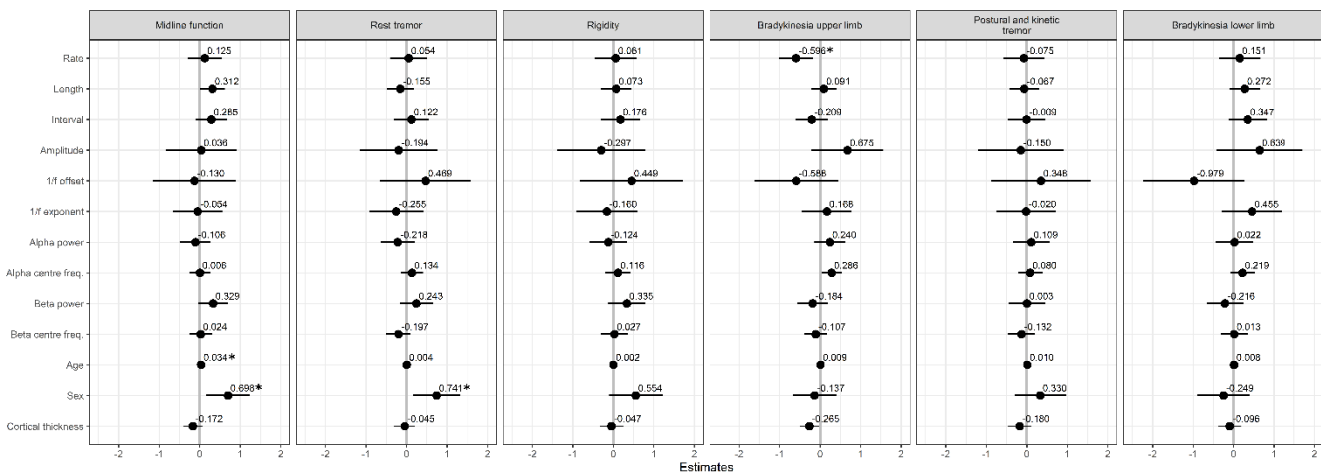
169 **Figure 5: Age-related differences in sensorimotor signal features.** Scatterplots of the individual
170 measures and model predictions over age for (A) burst rate, (B) PSD broadband 1/f intercept, and (C)
171 PSD broadband 1/f exponent, split between PD patients (blue) and healthy controls (red), and female
172 (solid) and male (dashed).

173 2.3 Clinical symptoms and oscillatory features

174 In the second analysis, we tested for associations between motor symptoms and the features of the
175 sensorimotor signal in the PD group. All sensorimotor signal features listed in Table 2 were used as
176 predictors in a multiple regression analysis that further included age, sex, and cortical thickness to
177 regress out the contribution hereof. The standardised regression coefficients of each predictor variable
178 on the motor symptoms measured with MDS-UPDRS-III⁵⁸ are presented in Figure 6.

179 Model comparison of multiple regression models showed evidence that burst rate was negatively
180 associated with upper limbs bradykinesia (BF = 12.70). The negative direction of the effect of burst
181 rate means that reduced burst rate was associated with increased severity of bradykinesia. The analysis
182 yielded no substantial evidence for effects of other sensorimotor signal features on symptom ratings for
183 axial symptoms, rest tremor, rigidity, rest tremor, postural/kinetic tremor, nor lower limb bradykinesia.

184 The analysis yielded substantial evidence for an effect of age on axial symptoms (BF = 5.79) and
 185 evidence for a difference between male and female patients on axial symptoms (BF = 7.56) and rest
 186 tremor (BF = 6.06). There were anecdotal evidence for an effect of alpha centre frequency on upper
 187 limbs bradykinesia (BF = 2.63), an effect of burst length on axial symptoms (BF = 1.49), as well as
 188 anecdotal evidence for an effect of cortical thickness on upper limbs bradykinesia (BF = 2.63).



189

190 **Figure 6: Regression analysis of motor symptoms.** Standardized regression coefficients for the
 191 regression analyses of sensorimotor signal features on clinical motor symptom ratings in PD. * indicate
 192 factors with Bayes Factor > 3 in the model comparison.

193 3 Discussion

194 This study aimed to explore how different features of cortical somatosensory oscillatory activity at rest
 195 differed between PD patients and healthy controls across age and gender and how these features relate
 196 to motor symptoms in PD. The analysis of spontaneous sensorimotor bursts showed an increased age-
 197 related reduction in PD patients compared to healthy controls. Notably, our current results show that

198 the reduced burst rate in PD is not a static group-level difference but interacts with age with a steeper
199 age-related reduction in burst rate in PD compared to healthy controls.

200 We hypothesised that different oscillatory features reflect distinct underlying functional neural
201 properties and manifest as different motor symptoms in PD. The results showed that a reduction in mu-
202 beta burst rate in PD was accompanied with an increase in bradykinesia severity, confirming previous
203 findings from our group.¹⁴ This relationship was exclusive for the bursts rate, as we observed no
204 statistically evident relationships between other burst features or PSD features and clinical motor
205 symptoms.

206 3.1 Characterizing neural time series data

207 The cortical sensorimotor activity of the PD patients differed from healthy controls, but did not differ
208 on the PSD in the canonical sensorimotor mu and beta bands. The PD patients showed a steeper
209 broadband 1/f slope and exponent of the broadband PSD than healthy controls. The observation of a
210 group difference in the spectral broadband 1/f characteristics of the signal adds to the growing evidence
211 that a focus on neural activity as narrow-band steady oscillations—e.g. narrowly focusing only on the
212 beta-band power—could potentially miss essential aspects of the neural signals for understanding
213 mechanistic changes in disease.^{59,60} Widening the quantitative analysis of PSD rather than focusing
214 exclusively on narrow band activity is of potential clinical value: quantifying only the peaks in the PSD
215 to differentiate patients from controls can misrepresent the actual oscillatory response at those
216 frequencies as the peaks are influenced by the broadband offset and 1/f exponent. Any unaccounted-for
217 systematic differences in either PSD offset or decay exponent can lead to a false conclusion that there
218 is a difference in the oscillatory response.^{51,52} Non-invasive measurements of changes in sensorimotor
219 activity is—despite the often conflicting findings⁴⁸—a potential useful method to assess disease-related

220 changes. At the current stage of the field there is, however, a need to further bridge how features in the
221 signals are linked to disease mechanisms.

222 Analysis of neural time series by frequency decomposition is a powerful tool to extract and summarise
223 features of the signal, but the method comes with limitations in what one can infer. In the time domain,
224 increased oscillatory power can reflect both increased burst duration and change in burst amplitude and
225 as an expression of true sustained oscillations in the signal.^{36,61} The presence of more sustained
226 oscillations in the sensorimotor rhythm might reflect a higher level of inhibition of sensorimotor
227 information; as is seen in recordings from STN⁵ and, to some extent, also at the cortical level.^{38,62}
228 However, sustained oscillations are not in contrast to the bursting properties of the sensorimotor
229 rhythm. The neural time-series can express both a degree of sustained oscillations while also exhibiting
230 variation in the degree of transient bursts—e.g., a signal of steady oscillation with transient high-
231 amplitude bursts.

232 3.2 Beta bursts and beta activity

233 Bursting properties of the cortical sensorimotor neural activity are proposed to occur due to long-range
234 input through the ascending thalamic-cortical connection to the cortex, leading to an increase in the
235 local neural excitation and resulting in a burst of synchronous activity.³⁶ The observed disease-related
236 changes in spontaneous cortical bursts, in the form of a more rapid decrease in rate over age for PD
237 patients, could reflect inhibition of these projections along the thalamic-cortical pathways caused by
238 disturbances in the dopamine-dependent structures projecting to the cortex. Interestingly, we did not
239 find significant group differences in burst duration in the current study—in line with previously
240 reported findings on cortical burst in PD¹⁴—supporting the view that the central mechanisms of the
241 cortical bursts are not primarily affected in PD—instead, it is the *rate* of bursts that is reduced at the

242 cortical level. The sub-cortical beta-band activity is influenced by the activity of dopamine-responding
243 neurons^{5,6,45}. The effect of dopamine and dopaminergic medication on the cortical beta-band is likely
244 mediated by the dopaminergic neurons projecting to the cortex that terminates in the pre-frontal cortex
245 but also to less extent in the primary sensorimotor cortex.⁶³ The differences in the cortical
246 sensorimotor burst rate in PD might be an indirect effect of the loss of dopamine and changes in the
247 beta band in the sub-cortical structures projecting to the sensorimotor cortex. The notion that the
248 cortical sensorimotor activity is indirectly related to dopamine depletion in PD is further supported by
249 findings from animals studies showing that 6-hydroxydopamine injections lead to exaggerated beta-
250 band oscillations only after several days had passed, suggesting that oscillatory changes occurred as an
251 indirect compensatory effect after dopamine depletion rather than a direct consequence of the depletion
252 itself.⁷ The indirect influence of dopamine on the cortical beta-band might also explain the often weak
253 or even absent effect of dopaminergic medication on cortical beta-band activity.^{11,13-15} The current
254 study cannot directly address the role of dopamine on cortical oscillations since all patients in the study
255 were tested on medication. However, a recent study found that cortical burst characteristics measured
256 with MEG were influenced by DBS therapy in PD and normalised the bursting characteristics during
257 DBS to resemble the burst characteristics of healthy controls.⁴⁶ This further supports that cortical
258 bursting activity is mediated by subthalamic projections.

259 3.3 Age-related differences

260 We explored how age-related differences in cortical sensorimotor neural activity might interact with
261 disease-related changes in PD. Age-related effects on spontaneous sensorimotor activity are commonly
262 dealt with by matching the age distributions of the patient group and the healthy control group—
263 usually within a narrow age span. The analysis showed age-related differences in burst rate, with PD

264 patients showing a more considerable reduction of burst as a function of age than healthy controls. The
265 steeper reduction in burst rate with age in PD seems in accordance with the fact that higher age at PD
266 onset is associated with a faster disease progression and more rapid decline in motor function⁶⁴, though
267 a longitudinal design is needed to confirm the relation between disease progression, reduction in burst
268 rate, and age. We did not see a significant "slowing" of the beta PSD centre frequency between groups,
269 as reported in several previous studies.⁴⁸ An explanation might be that such slowing is more
270 pronounced in PD patients with dementia²⁷⁻³⁰ and correlates with cognitive ability.²⁶ The PD patients in
271 the current study did not differ in their cognitive ability from the healthy controls. Furthermore, we
272 focused on the activity in the sensorimotor cortex, whereas the slowing of alpha and beta PSD is
273 usually found in frontal areas and globally throughout the brain.^{25,28,31} We included cortical thickness
274 measures within the same ROI from which we extracted the functional time-series, as we hypothesised
275 that age-related effects upon the functional measures might be mediated through the age-related
276 structural changes in the cortex. However, despite the negative correlation between age and cortical
277 thickness (see supplementary material), we did not find pervasive evidence that cortical thickness
278 affected any of the functional measures.

279 3.4 Sex differences

280 We also included sex to explore if disease-related changes in sensorimotor oscillatory activity differed
281 between males and females, as there are well-documented sex differences in the manifestation of
282 PD.^{1,65} Male sex is a risk factor for developing PD, with an average incidence ratio of approximately
283 2:1 male-female ratio across all stages of the disease.⁶⁶ The disease onset is on average two years
284 earlier in males than females and differs in the initial manifestation of symptoms, with women more
285 likely to develop tremor specific symptoms and men more likely to develop rigidity.⁶⁷ We are not

286 aware of any previous studies that explicitly included sex as a factor in analysing neural oscillations in
287 PD. The regression analysis of motor symptoms showed evidence for a difference in midline function
288 and rest tremor between male and female patients. We did not, however, find widespread sex
289 differences in the various features of the sensorimotor activity. The analysis of the sensorimotor signal
290 features only showed evidence for differences between males and females in the burst rate. A possible
291 factor behind the sex differences in PD is the contribution of sex hormones on the nigrostriatal pathway
292 and linked to the deterioration of the dopaminergic system, where testosterone levels appear to enhance
293 dopamine loss, while estrogen has been identified as a neuroprotective agent for PD. Estrogen has been
294 demonstrated to influence incidence levels of PD while menopause-related variations in estrogen levels
295 are linked to variations in PD symptom severity.⁶⁸ At the current stage, it is unclear if estrogen sex
296 hormones influences oscillatory bursts in the sensorimotor cortex. These findings illustrate the need for
297 further studies into sex-specific changes in neural function and how they manifest and relate to PD.

298 3.5 Limitations and conclusions

299 The present study quantified the neural time series from the sensorimotor cortex based on pre-defined
300 summary measures of its PSD and burst properties. We included more PD patients and healthy controls
301 than similar previously conducted functional studies—typically in the range of 5-30 participants.⁴⁸ A
302 limitation of our study for understanding the extent of changes in oscillatory sensorimotor activity is
303 the focus on different features within a narrow ROI, which ignores other types of measurements that
304 are potentially relevant to understanding the development of PD and motor symptoms: for example, the
305 long-range connectivity between the sensorimotor cortex and other cortical areas and the connections
306 between the sensorimotor cortex and the basal ganglia and thalamus (though the subcortical structures
307 are practically invisible in MEG).

308 Treating the activity in the sensorimotor cortex as single time series also means that we remove the
309 sensitivity to spatial features of the signals, e.g., focal versus spatially blurred activity in one group or
310 the other. If the oscillatory activity extends over a larger cortical surface area, that signal will also
311 manifest as power differences in the measured signal.⁶¹ There are potentially other features to be
312 uncovered, and future studies may explore how the PSD- and burst features further interact with other
313 aspects of brain activity in the global function of the brain to fully understand the interaction between
314 functional and structural changes in PD.

315 We investigated a relatively large cohort of PD patients and healthy controls (for a neuroimaging
316 study) to make meaningful inferences about how age and sex interact with the group level difference
317 between PD patients and healthy controls; however, a limitation is that our study is cross-sectional. We
318 aim to follow this cohort longitudinally to estimate the development trajectories of the sensorimotor
319 oscillatory activity in PD compared to healthy ageing.

320 Sensorimotor activity measured non-invasively with MEG/EEG contains rich information about the
321 functional state of the sensorimotor system and how it changes in PD. The central challenge is
322 quantifying the measured neural signals to extract the disease's relevant features from the signals, be it
323 the spectral power, centre frequencies, or burst-like features. Finding features of neural signals that can
324 explain disease mechanism or symptoms, even if extracted along with a reduced number of dimensions,
325 will be helpful if they provide adequate information about the disease- or symptom-state. Further
326 characterisation of the association between features in the non-invasive brain signals and motor
327 symptoms can potentially be a valuable tool to aid in diagnosis and treatment evaluation.

328 Understanding how features in the neural time series are related to motor symptoms in PD will also
329 help develop non-invasive neural stimulation that can potentially relieve motor symptoms.^{37,69}

330 4 Methods

331 4.1 Participants

332 Eighty PD patients (age 44-85; 32 female) and 71 healthy controls (age 46–78; 46 female) participated
333 in the study. The study was approved by the regional ethics committee (Etikprövningsnämnden
334 Stockholm, DNR 2019-00542) and followed the Declaration of Helsinki. All participants gave written
335 informed consent before participation.

336 The PD patients were recruited from the Parkinson's Outpatient Clinic, Department of Neurology,
337 Karolinska University Hospital, Stockholm, Sweden. The healthy controls were recruited by
338 advertising or amongst spouses of PD patients. 22 participants (18 patients, 4 healthy controls) were
339 included from a previous study¹⁴ who were qualified based on the recruitment criteria of the present
340 study and had done the same MEG and MRI procedures as in the present study. All data were
341 reanalysed following the procedure described below.

342 The inclusion criteria for the PD group were a diagnosis of PD according to the United Kingdom
343 Parkinson's Disease Society Brain Bank Diagnostic Criteria with Hoehn and Yahr stage 1-3.⁷⁰
344 Inclusion criteria for the control group were not having a diagnosis of PD, no form of movement
345 disorder, and no history of neurological disorders, epilepsy, or psychiatric disorders.

346 Exclusion criteria for both groups were a diagnosis of major depression, dementia, history or presence
347 of schizophrenia, bipolar disorder, epilepsy, or history of alcoholism or drug addiction according to the
348 *Diagnostic and Statistical Manual of Mental Disorders*.⁷¹

349 One participant declined to do the MRI scanning, one participant had a scanner malfunction during
350 MRI acquisition, and 11 participants had their MRI scans cancelled due to the Covid-19 pandemic and

351 were not included in the analysis. In total, two PD patients and 11 healthy controls were excluded from
352 the analysis. Table 1 is a summary of the participants included in the analysis.

353 The PD patients participated in the study while on their regular prescribed dose of medication. The
354 levodopa equivalent daily dose (LEDD) was calculated according to Tomlinson et al.⁷² Motor
355 symptoms in the PD group were assessed using the motor section of the Movement-Disorder Society
356 Unified Parkinson's Disease Rating Scale (MDS-UPDRS-III).⁵⁹ Global cognition was assessed with the
357 Montreal Cognitive Assessment battery (MoCA).⁷⁴

358 4.2 MEG recordings

359 MEG data were recorded with a Neuromag TRIUX 306-channel MEG system, with 102
360 magnetometers and 102 pairs of planar gradiometers. Data were sampled at 1000 Hz with an online 0.1
361 Hz high-pass filter and 330 Hz low-pass filter. The MEG scanner was located inside a two-layer
362 magnetically shielded room (Vacuumschmelze GmbH) with internal active shielding active to suppress
363 electromagnetic artefacts. The subjects' head position and head movements inside the MEG scanner
364 were measured during recordings with head-position indicator coils (HPI) attached to subjects' heads.
365 The HPI location and additional points sampled uniformly across the subjects' head shape were
366 digitalised with a Polhemus Fastrak motion tracker before the measurements. Horizontal and vertical
367 electrooculogram (EOG) and electrocardiogram (ECG) were recorded simultaneously with the MEG.
368 We recorded three minutes of resting-state MEG while the participants sat with their eyes closed. The
369 participants were instructed to close their eyes and relax. The recordings began after assuring the
370 participant sat still with their eyes closed.

371 4.3 MRI acquisition

372 3D T1-weighted magnetisation-prepared rapid gradient-echo (MPRAGE) sequence structural images
373 (voxel size: 1x1x1 mm) were obtained on a GE Discovery 3.0 T MR scanner for morphological
374 analysis and creating source spaces for MEG source reconstruction. Multi-echo "FLASH"⁷⁵ images
375 were obtained to create volumetric headmodels for MEG source reconstruction (see below).

376 4.4 MRI processing

377 The MRI images were processed with Freesurfer⁷⁶ (v. 5.3) to get surface reconstructions of the cortical
378 mantle. The surfaces were obtained with the automatic routine for extracting cortical surfaces in
379 Freesurfer from the individual T1-weighted MRI.

380 We defined the cortical sensorimotor area by segmenting the cortical surface using the anatomical
381 labels provided by Freesurfer automatic labelling.⁷⁷ The analysis focused on a region of interest (ROI)
382 consisting of the left pre- and post-central gyri and central sulcus. The pre/postcentral gyri were
383 combined because a biomagnetic source on either sulci wall will leave a trace on the other side due to
384 the close distance and the field spread of MEG signals. The ROI was defined for each subject based on
385 the individual cortical reconstructions. The average cortical thickness in the ROI was estimated with
386 Freesurfer.⁷⁸

387 4.5 MEG pre-processing

388 The MEG data was processed by applying temporal signal space separation (tSSS) to suppress artefacts
389 from outside the scanner helmet and correct head movement during the recording.⁷⁹ The tSSS had a
390 buffer length of 10 s and a cut-off correlation coefficient of 0.95. Movement correction was done by

391 shifting the head position to a position based on the median of the continuous head position during the
392 three-minute recording.

393 The MEG data processing and source reconstruction was done with MNE-Python⁸⁰ in Python 3.8. First,
394 we marked data segments containing muscle artefacts and SQUID jumps with the automatic artefact
395 detection in MNE-Python. The data was filtered with a 48 Hz low-pass filter and 50 Hz notch filter to
396 remove line noise. The continuous data were cut into 1.0 s epochs, and epochs with muscle artefacts or
397 extreme values (5000 fT for magnetometers and 4000 fT/cm for gradiometers) were rejected. Between
398 0-65 % (median: 6.0 %) of data was rejected resulting in 63.0-180 s (median: 174.0 s) of useful MEG
399 data per participant. The remaining data length was not significantly different between groups
400 (Wilcoxon rank sum test, $p = 0.98$). We then performed an independent component analysis (ICA)
401 using the *fastica* algorithm⁸¹ to identify artefacts from blinks and heartbeats. Components showing
402 correlation with the EOG and ECG were removed from the raw data. Between 0-5 (median 3)
403 components were removed per participant. The number of removed ICA components was not
404 significantly different between groups (Wilcoxon rank sum test, $p = 0.71$).

405 We then applied source reconstruction using noise weighted minimum-norm estimates.⁸² The noise
406 covariance matrix was estimated from two minutes of empty room MEG data recorded before each
407 session. The source space consisted of 5124 evenly spaced points sampled across the white matter
408 surfaces. The inner skull boundary was estimated from the multi-echo MRI to create a single shell
409 volume conductor model. The time series from the sensorimotor ROI (see Figure. 1) was extracted
410 from the estimated source time series by singular value decomposition of all source points within the
411 ROI.

412 4.6 Power spectral analysis

413 We analysed the spectral properties of the sensorimotor activity by calculating the PSD from 0.5 to 40
414 Hz across the entire cleaned ROI time series using Welch's method by segmenting the continuous data
415 into 3.072 s epochs with 50% overlap and averaging the PSD across the segments.

416 Since the narrow-band beta power in the PSD is dependent on the broader features of the broadband
417 spectrum, we further analysed the 1/f broadband characteristic of the sensorimotor activity as this could
418 play a role in the functional properties of the beta-band and has been shown to differ between healthy
419 control and PD patients.¹⁴ We used the *fitting oscillations & one over f* (FOOOF) toolbox⁵¹ to analyse
420 the 1/f broadband characteristic of the PSD (intercept and exponent) and the oscillatory peaks in the
421 canonically defined beta band (13-30 Hz) and alpha band (8-12 Hz). A log-linear regression is fitted to
422 the PSD and subtracted before fitting Gaussian functions to the peaks in the PSD. The midpoint of the
423 Gaussian function fitted to a given frequency band corresponds to the peak frequency in that frequency
424 band and the height represents the signal power. A new log-linear function is fitted to the PSD after
425 subtracting the Gaussian function to estimate the 1/f characteristic.

426 All participants showed a discernible beta peak in the PSD. Nine PD patients and nine healthy controls
427 did not show a peak in the PSD alpha band (no difference between groups, $\chi^2(1) = 0.12$; $p = 0.73$).

428 4.7 Burst analysis

429 To calculate the burst properties of the sensorimotor activity in the time domain, we band-pass filtered
430 the time-series with an 8-30 Hz band-pass filter using FieldTrip⁸³ in MATLAB (R2016b; MathWorks
431 Inc.) and calculated the Hilbert envelope of the signal. The burst threshold was defined as two times the
432 median of the signal. The burst onset was defined as the time-point where the signal first reached half
433 the max amplitude of the burst and ended at the time-point where the signal again dropped below half

434 the max amplitude of the burst. The *burst amplitude* was defined as the maximum value of the burst.
435 The *burst duration* was defined as the time from burst onset to burst end. The *burst interval* was
436 defined as the time from the end of a burst to the time-point where the next burst began.

437 4.8 Statistics

438 4.8.1 Analysis of sensorimotor rhythm features

439 The main analyses tested the effect of *group* (PD patients/healthy controls), *age*, *sex*, and *ROI cortical*
440 *thickness* on the features listed in Table 2. For the PSD features, we modelled the outcomes as a linear
441 function of group (PD patients/healthy controls), age, age squared, sex, and cortical thickness with
442 linear regression in *R* (v. 4.0.2).⁸⁴ The regression models were fitted to the data for each participant
443 with all factors and up to their three-way interactions between the four predictors. Gaussian regression
444 models were estimated for each feature, except for the burst rate (burst per minute), which was
445 modelled with Poisson regression using the same predictor variables. Before fitting the regression
446 models, burst duration, burst interval, and burst amplitude were log-transformed.

447 Significance testing was done by removing one predictor from the model and comparing the variance
448 explained between the full model and the model with a predictor removed. Hypothesis testing was done
449 by computing the Bayes factor (BF) for the model with a given predictor (H1) versus the model
450 without the predictor (H0) using the BIC approximation.⁸⁵ The BF tells how much more likely the
451 observed data is under the alternative model (H1) versus the null model (H0). The Bayesian model
452 comparison, therefore, avoids the multiple comparison problem of frequentist hypothesis testing
453 (theoretical likelihood of the hypothesis given the observed data). The model comparison approach
454 furthermore circumvents issues with the interpretation of p-values of individual regression coefficients
455 due to internal correlation between predictor variables. Following the conventional interpretation of

456 BFs, we used $BF > 3$ as a cut-off between anecdotal evidence and substantial effects.⁵⁷ The BFs for all
457 comparisons are presented in Supplementary Table S3.

458 4.8.2 Clinical scores and sensorimotor oscillatory features

459 The MDS-UPDRS-III scores were divided into subscales based on symptoms: *midline function, rest*
460 *tremor, rigidity, upper-body bradykinesia, postural and kinetic tremor, and lower limb bradykinesia*;
461 according to Goetz et al.⁸⁶, with the exception that left- and right-side upper-body bradykinesia were
462 combined into a single factor.

463 Each symptom score was analysed by multiple regression and modelled as a function of the burst rate,
464 median burst duration, median bursts interval, median burst amplitude, PSD 1/f intercept, PSD 1/f
465 exponent, PSD beta power, PSD beta centre frequency, PSD alpha power, and PSD alpha centre
466 frequency for each PD patient. The models further included the age, sex, and cortical thickness to
467 regress out the contribution hereof and estimate the relative effect size of each signal feature. All
468 symptom ratings and continuous predictor variables, except age, were z-transformed to get the
469 standardised effect size. Significance testing was done by removing one predictor from the model and
470 calculating the BF between the full model (H1) and the model without the predictor (H0) using the BIC
471 approximation for BFs. The BFs for all comparisons are presented in Supplementary Table S4.

472 4.9 Data Availability

473 The full dataset cannot be made publicly available, as the ethical permits for the study does not allow
474 for open data sharing. Parts of the data used in this analysis will be made available as part of an online
475 data repository (Vinding, et al. *in prep*). The scripts used to process the data and run the analysis
476 presented in the paper are available at: https://github.com/natmegsweden/PD_beta_bursts2.

477 Authorship contribution statement

478 **Mikkel C. Vinding**: conceptualization, methodology, software, validation, formal analysis,
479 investigation, data curation, writing - original draft, writing - review & editing, project administration.
480 **Allison Eriksson**: investigation, resources, data curation, writing - review & editing, project
481 administration. **Cassia Man Ting Low**: investigation, writing - review & editing. **Josefine**
482 **Waldthaler**: investigation, writing - review & editing. **Daniel Ferreira**: supervision, writing - review
483 & editing. **Martin Ingvar**: conceptualization, writing - review & editing, resources, funding
484 acquisition. **Per Svenningsson**: conceptualization, methodology, resources, supervision, data curation,
485 writing - review & editing, Project administration, Funding acquisition. **Daniel Lundqvist**:
486 conceptualization, methodology, formal analysis, resources, supervision, writing - original draft,
487 writing - review & editing, project administration, funding acquisition.

488 Declaration of competing Interest

489 The authors declare that they have no known competing financial interests or personal relationships
490 that could have appeared to influence the work reported in this paper.

491 References

- 492 1. Kalia, L. V. & Lang, A. E. Parkinson's disease. *The Lancet* **386**, 896–912 (2015).
- 493 2. Rodriguez-Oroz, M. C. *et al.* Initial clinical manifestations of Parkinson's disease: features and
494 pathophysiological mechanisms. *The Lancet Neurology* **8**, 1128–1139 (2009).
- 495 3. Braak, H. *et al.* Staging of brain pathology related to sporadic Parkinson's disease. *Neurobiology of*
496 *aging* **24**, 197–211 (2003).
- 497 4. Jenkinson, N. & Brown, P. New insights into the relationship between dopamine, beta oscillations
498 and motor function. *Trends in Neurosciences* **34**, 611–618 (2011).
- 499 5. Alonso-Frech, F. *et al.* Slow oscillatory activity and levodopa-induced dyskinesias in Parkinson's
500 disease. *Brain* **129**, 1748–1757 (2006).
- 501 6. Giannicola, G. *et al.* The effects of levodopa and ongoing deep brain stimulation on subthalamic
502 beta oscillations in Parkinson's disease. *Experimental Neurology* **226**, 120–127 (2010).
- 503 7. Mallet, N. *et al.* Disrupted Dopamine Transmission and the Emergence of Exaggerated Beta
504 Oscillations in Subthalamic Nucleus and Cerebral Cortex. *Journal of Neuroscience* **28**, 4795–4806
505 (2008).
- 506 8. Neumann, W.-J. *et al.* Long term correlation of subthalamic beta band activity with motor
507 impairment in patients with Parkinson's disease. *Clinical Neurophysiology* **128**, 2286–2291 (2017).
- 508 9. Kühn, A. A., Kupsch, A., Schneider, G.-H. & Brown, P. Reduction in subthalamic 8-35 Hz
509 oscillatory activity correlates with clinical improvement in Parkinson's disease: STN activity and
510 motor improvement. *European Journal of Neuroscience* **23**, 1956–1960 (2006).

- 511 10. Martin, S. *et al.* Differential contributions of subthalamic beta rhythms and 1/f broadband activity
512 to motor symptoms in Parkinson's disease. *npj Parkinson's Disease* **4**, 32 (2018).
- 513 11. Airaksinen, K. *et al.* Somatomotor mu rhythm amplitude correlates with rigidity during deep brain
514 stimulation in Parkinsonian patients. *Clinical Neurophysiology* **123**, 2010–2017 (2012).
- 515 12. Feldmann, L. K. *et al.* Subthalamic beta band suppression reflects effective neuromodulation in
516 chronic recordings. *European Journal of Neurology* ene.14801 (2021) doi:10.1111/ene.14801.
- 517 13. Hall, S. D. *et al.* GABA-mediated changes in inter-hemispheric beta frequency activity in early-
518 stage Parkinson's disease. *Neuroscience* **281**, 68–76 (2014).
- 519 14. Vinding, M. C. *et al.* Reduction of spontaneous cortical beta bursts in Parkinson's disease is linked
520 to symptom severity. *Brain Communications* (2020) doi:10.1093/braincomms/fcaa052.
- 521 15. Vinding, M. C. *et al.* Attenuated beta rebound to proprioceptive afferent feedback in Parkinson's
522 disease. *Scientific Reports* **9**, (2019).
- 523 16. Cao, C. *et al.* L-dopa treatment increases oscillatory power in the motor cortex of Parkinson's
524 disease patients. *NeuroImage: Clinical* **26**, 102255 (2020).
- 525 17. Heinrichs-Graham, E. *et al.* Hypersynchrony despite pathologically reduced beta oscillations in
526 patients with Parkinson's disease: a pharmaco-magnetoencephalography study. *Journal of*
527 *Neurophysiology* **112**, 1739–1747 (2014).
- 528 18. Melgari, J.-M. *et al.* Alpha and beta EEG power reflects L-dopa acute administration in
529 parkinsonian patients. *Frontiers in Aging Neuroscience* **6**, 302 (2014).
- 530 19. Abbasi, O. *et al.* Unilateral deep brain stimulation suppresses alpha and beta oscillations in
531 sensorimotor cortices. *NeuroImage* **174**, 201–207 (2018).

- 532 20. Luoma, J. *et al.* Spontaneous sensorimotor cortical activity is suppressed by deep brain stimulation
533 in patients with advanced Parkinson's disease. *Neuroscience Letters* **683**, 48–53 (2018).
- 534 21. Cao, C.-Y. *et al.* Modulations on cortical oscillations by subthalamic deep brain stimulation in
535 patients with Parkinson disease: A MEG study. *Neuroscience Letters* **636**, 95–100 (2017).
- 536 22. Pollok, B. *et al.* Motor-cortical oscillations in early stages of Parkinson's disease: Suppression of
537 motor cortical beta oscillations is altered in early PD. *The Journal of Physiology* **590**, 3203–3212
538 (2012).
- 539 23. Olde Dubbelink, K. T. E. *et al.* Resting-state functional connectivity as a marker of disease
540 progression in Parkinson's disease: A longitudinal MEG study. *NeuroImage: Clinical* **2**, 612–619
541 (2013).
- 542 24. Boon, L. I. *et al.* Motor effects of deep brain stimulation correlate with increased functional
543 connectivity in Parkinson's disease: An MEG study. *NeuroImage: Clinical* **26**, 102225 (2020).
- 544 25. Stoffers, D. *et al.* Slowing of oscillatory brain activity is a stable characteristic of Parkinson's
545 disease without dementia. *Brain* **130**, 1847–1860 (2007).
- 546 26. Vardy, A. N. *et al.* Slowing of M1 activity in Parkinson's disease during rest and movement – An
547 MEG study. *Clinical Neurophysiology* **122**, 789–795 (2011).
- 548 27. Bosboom, J. L. W., Stoffers, D., Wolters, E. Ch., Stam, C. J. & Berendse, H. W. MEG resting state
549 functional connectivity in Parkinson's disease related dementia. *Journal of Neural Transmission*
550 **116**, 193–202 (2009).
- 551 28. Bosboom, J. L. W. *et al.* Resting state oscillatory brain dynamics in Parkinson's disease: An MEG
552 study. *Clinical Neurophysiology* **117**, 2521–2531 (2006).

- 553 29. Olde Dubbelink, K. T. E. *et al.* Predicting dementia in Parkinson disease by combining
554 neurophysiologic and cognitive markers. *Neurology* **82**, 263–270 (2014).
- 555 30. Ponsen, M. M., Stam, C. J., Bosboom, J. L. W., Berendse, H. W. & Hillebrand, A. A three
556 dimensional anatomical view of oscillatory resting-state activity and functional connectivity in
557 Parkinson’s disease related dementia: An MEG study using atlas-based beamforming.
558 *NeuroImage: Clinical* **2**, 95–102 (2013).
- 559 31. Olde Dubbelink, K. T. E. *et al.* Cognitive decline in Parkinson’s disease is associated with slowing
560 of resting-state brain activity: a longitudinal study. *Neurobiology of Aging* **34**, 408–418 (2013).
- 561 32. Stoffers, D., Bosboom, J. L. W., Wolters, E. Ch., Stam, C. J. & Berendse, H. W. Dopaminergic
562 modulation of cortico-cortical functional connectivity in Parkinson’s disease: An MEG study.
563 *Experimental Neurology* **213**, 191–195 (2008).
- 564 33. Karekal, A., Miocinovic, S. & Swann, N. C. Novel approaches for quantifying beta synchrony in
565 Parkinson’s disease. *Exp Brain Res* **240**, 991–1004 (2022).
- 566 34. Feingold, J., Gibson, D. J., DePasquale, B. & Graybiel, A. M. Bursts of beta oscillation
567 differentiate postperformance activity in the striatum and motor cortex of monkeys performing
568 movement tasks. *Proc. Natl. Acad. Sci. U.S.A.* **112**, 13687–13692 (2015).
- 569 35. Leventhal, D. K. *et al.* Basal Ganglia Beta Oscillations Accompany Cue Utilization. *Neuron* **73**,
570 523–536 (2012).
- 571 36. Sherman, M. A. *et al.* Neural mechanisms of transient neocortical beta rhythms: Converging
572 evidence from humans, computational modeling, monkeys, and mice. *Proceedings of the National*
573 *Academy of Sciences* **113**, E4885–E4894 (2016).

- 574 37. Tinkhauser, G. *et al.* The modulatory effect of adaptive deep brain stimulation on beta bursts in
575 Parkinson's disease. *Brain* **140**, 1053–1067 (2017).
- 576 38. Shin, H., Law, R., Tsutsui, S., Moore, C. I. & Jones, S. R. The rate of transient beta frequency
577 events predicts behavior across tasks and species. *eLife* **6**, (2017).
- 578 39. Duchet, B. *et al.* Average beta burst duration profiles provide a signature of dynamical changes
579 between the ON and OFF medication states in Parkinson's disease.
580 <http://biorxiv.org/lookup/doi/10.1101/2020.04.27.064246> (2020) doi:10.1101/2020.04.27.064246.
- 581 40. Khawaldeh, S. *et al.* Subthalamic nucleus activity dynamics and limb movement prediction in
582 Parkinson's disease. *Brain* **143**, 582–596 (2020).
- 583 41. Lofredi, R. *et al.* Beta bursts during continuous movements accompany the velocity decrement in
584 Parkinson's disease patients. *Neurobiology of Disease* (2019) doi:10.1016/j.nbd.2019.03.013.
- 585 42. Little, S., Bonaiuto, J., Barnes, G. & Bestmann, S. Human motor cortical beta bursts relate to
586 movement planning and response errors. *PLoS Biol* **17**, e3000479 (2019).
- 587 43. Brady, B., Power, L. & Bardouille, T. Age-related trends in neuromagnetic transient beta burst
588 characteristics during a sensorimotor task and rest in the Cam-CAN open-access dataset.
589 *NeuroImage* **222**, 117245 (2020).
- 590 44. Tinkhauser, G. *et al.* Beta burst coupling across the motor circuit in Parkinson's disease.
591 *Neurobiology of Disease* **117**, 217–225 (2018).
- 592 45. Tinkhauser, G. *et al.* Beta burst dynamics in Parkinson's disease OFF and ON dopaminergic
593 medication. *Brain* **140**, 2968–2981 (2017).

- 594 46. Pauls, K. A. M. *et al.* Cortical beta burst dynamics are altered in Parkinson's disease but
595 normalized by deep brain stimulation. *NeuroImage* 119308 (2022)
596 doi:10.1016/j.neuroimage.2022.119308.
- 597 47. Power, L. & Bardouille, T. Age-related trends in the cortical sources of transient beta bursts
598 during a sensorimotor task and rest. *NeuroImage* **245**, 118670 (2021).
- 599 48. Boon, L. I. *et al.* A systematic review of MEG-based studies in Parkinson's disease: The motor
600 system and beyond. *Hum Brain Mapp* **40**, 2827–2848 (2019).
- 601 49. Salmelin, R., Hämäläinen, M., Kajola, M. & Hari, R. Functional Segregation of Movement-Related
602 Rhythmic Activity in the Human Brain. *NeuroImage* **2**, 237–243 (1995).
- 603 50. Salmelin, R. & Hari, R. Spatiotemporal characteristics of sensorimotor neuromagnetic rhythms
604 related to thumb movement. *Neuroscience* **60**, 537–550 (1994).
- 605 51. Donoghue, T. *et al.* Parameterizing neural power spectra into periodic and aperiodic components.
606 *Nat Neurosci* **23**, 1655–1665 (2020).
- 607 52. He, B. J., Zempel, J. M., Snyder, A. Z. & Raichle, M. E. The Temporal Structures and Functional
608 Significance of Scale-free Brain Activity. *Neuron* **66**, 353–369 (2010).
- 609 53. Bardouille, T., Bailey, L. & CamCAN Group. Evidence for age-related changes in sensorimotor
610 neuromagnetic responses during cued button pressing in a large open-access dataset. *NeuroImage*
611 **193**, 25–34 (2019).
- 612 54. Wolpe, N. *et al.* Ageing increases reliance on sensorimotor prediction through structural and
613 functional differences in frontostriatal circuits. *Nature Communications* **7**, (2016).

- 614 55. Yau, Y. *et al.* Network connectivity determines cortical thinning in early Parkinson's disease
615 progression. *Nat Commun* **9**, 12 (2018).
- 616 56. Lyoo, C. H., Ryu, Y. H. & Lee, M. S. Cerebral cortical areas in which thickness correlates with
617 severity of motor deficits of Parkinson's disease. *J Neurol* **258**, 1871–1876 (2011).
- 618 57. Wetzels, R. *et al.* Statistical Evidence in Experimental Psychology An Empirical Comparison
619 Using 855 t Tests. *Perspectives on Psychological Science* **6**, 291–298 (2011).
- 620 58. Goetz, C. G. *et al.* Movement Disorder Society-sponsored revision of the Unified Parkinson's
621 Disease Rating Scale (MDS-UPDRS): Process, format, and clinimetric testing plan. *Movement*
622 *Disorders* **22**, 41–47 (2007).
- 623 59. Robertson, M. M. *et al.* EEG power spectral slope differs by ADHD status and stimulant
624 medication exposure in early childhood. *Journal of Neurophysiology* **122**, 2427–2437 (2019).
- 625 60. Gao, R., Peterson, E. J. & Voytek, B. Inferring synaptic excitation/inhibition balance from field
626 potentials. *NeuroImage* **158**, 70–78 (2017).
- 627 61. Zich, C., Quinn, A. J., Mardell, L. C., Ward, N. S. & Bestmann, S. Dissecting Transient Burst
628 Events. *Trends in Cognitive Sciences* S136466132030173X (2020) doi:10.1016/j.tics.2020.07.004.
- 629 62. Muralidharan, V. & Aron, A. R. Behavioral Induction of a High Beta State in Sensorimotor Cortex
630 Leads to Movement Slowing. *Journal of Cognitive Neuroscience* 1–18 (2021)
631 doi:10.1162/jocn_a_01717.
- 632 63. Luft, A. R. & Schwarz, S. Dopaminergic signals in primary motor cortex. *Int. j. dev. neurosci.* **27**,
633 415–421 (2009).

- 634 64. De Pablo-Fernández, E., Lees, A. J., Holton, J. L. & Warner, T. T. Prognosis and Neuropathologic
635 Correlation of Clinical Subtypes of Parkinson Disease. *JAMA Neurol* **76**, 470 (2019).
- 636 65. Göttgens, I. *et al.* The Impact of Sex and Gender on the Multidisciplinary Management of Care for
637 Persons With Parkinson’s Disease. *Frontiers in Neurology* **11**, (2020).
- 638 66. Elbaz, A. *et al.* Risk tables for parkinsonism and Parkinson’s disease. *Journal of Clinical*
639 *Epidemiology* **55**, 25–31 (2002).
- 640 67. Georgiev, D., Hamberg, K., Hariz, M., Forsgren, L. & Hariz, G.-M. Gender differences in
641 Parkinson’s disease: A clinical perspective. *Acta Neurol Scand* **136**, 570–584 (2017).
- 642 68. Gillies, G. E., Pienaar, I. S., Vohra, S. & Qamhawi, Z. Sex differences in Parkinson’s disease.
643 *Frontiers in Neuroendocrinology* **35**, 370–384 (2014).
- 644 69. Cook, A. J., Pfeifer, K. J. & Tass, P. A. A Single Case Feasibility Study of Sensorimotor Rhythm
645 Neurofeedback in Parkinson’s Disease. *Front. Neurosci.* **15**, 623317 (2021).
- 646 70. Hoehn, M. M. & Yahr, M. D. Parkinsonism: onset, progression, and mortality. *Neurology* **17**, 427–
647 427 (1967).
- 648 71. American Psychiatric Association. *Diagnostic and Statistical Manual of Mental Disorders*.
649 (American Psychiatric Publishing, 2013).
- 650 72. Tomlinson, C. L. *et al.* Systematic review of levodopa dose equivalency reporting in Parkinson’s
651 disease. *Movement Disorders* (2010) doi:10.1002/mds.23429.
- 652 73. Goetz, C. G. *et al.* Movement disorder society-sponsored revision of the unified Parkinson’s
653 disease rating scale (MDS-UPDRS): Process, format, and clinimetric testing plan. *Movement*
654 *Disorders* (2007) doi:10.1002/mds.21198.

- 655 74. Nasreddine, Z. S. *et al.* The Montreal Cognitive Assessment, MoCA: a brief screening tool for mild
656 cognitive impairment. *Journal of the American Geriatrics Society* **53**, 695–699 (2005).
- 657 75. Fischl, B. *et al.* Sequence-independent segmentation of magnetic resonance images. *NeuroImage*
658 **23**, S69–S84 (2004).
- 659 76. Dale, A. M., Fischl, B. & Sereno, M. I. Cortical Surface-Based Analysis: I. segmentation and
660 surface reconstruction. *NeuroImage* **9**, 179–194 (1999).
- 661 77. Destrieux, C., Fischl, B., Dale, A. & Halgren, E. Automatic parcellation of human cortical gyri and
662 sulci using standard anatomical nomenclature. *NeuroImage* **53**, 1–15 (2010).
- 663 78. Fischl, B. & Dale, A. M. Measuring the thickness of the human cerebral cortex from magnetic
664 resonance images. *Proceedings of the National Academy of Sciences* **97**, 11050–11055 (2000).
- 665 79. Taulu, S. & Simola, J. Spatiotemporal signal space separation method for rejecting nearby
666 interference in MEG measurements. *Physics in Medicine and Biology* **51**, 1759–1768 (2006).
- 667 80. Gramfort, A. *et al.* MEG and EEG data analysis with MNE-Python. *Frontiers in Neuroscience* **7**,
668 267 (2013).
- 669 81. Hyvarinen, A. Fast and robust fixed-point algorithms for independent component analysis. *IEEE*
670 *Transactions on Neural Networks* **10**, 626–634 (1999).
- 671 82. Dale, A. M. *et al.* Dynamic Statistical Parametric Mapping: Combining fMRI and MEG for High-
672 Resolution Imaging of Cortical Activity. *Neuron* **26**, 55–67 (2000).
- 673 83. Oostenveld, R., Fries, P., Maris, E. & Schoffelen, J.-M. FieldTrip: Open Source Software for
674 Advanced Analysis of MEG, EEG, and Invasive Electrophysiological Data. *Computational*
675 *Intelligence and Neuroscience* **2011**, 1–9 (2011).

- 676 84. R Core Team. *R: A Language and Environment for Statistical Computing*. (R Foundation for
677 Statistical Computing, 2020).
- 678 85. Wagenmakers, E.-J. A practical solution to the pervasive problems of p values. *Psychonomic*
679 *Bulletin & Review* **14**, 779–804 (2007).
- 680 86. Goetz, C. G. *et al.* Movement Disorder Society-sponsored revision of the Unified Parkinson’s
681 Disease Rating Scale (MDS-UPDRS): Scale presentation and clinimetric testing results. *Movement*
682 *Disorders* **23**, 2129–2170 (2008).
- 683

1 Figure legends

2 Figure 1: Overview of the data processing pipeline.

3 Three minutes raw resting-state MEG data was obtained from each participant. The signals were
4 projected through a minimum-norm source reconstruction to extract the activity in the sensorimotor
5 cortex. We did a frequency decomposition of the source reconstructed signal to calculate the PSD to
6 which a 1/f and Gaussian curve were fitted to extract the PSD features (Table 2). In addition, we
7 quantified sensorimotor bursts in the signal time series in the sensorimotor ROI by thresholding the
8 envelope of the band-pass filtered (8-30 Hz) signal to the mu-beta frequency range.

9 Figure 2: Group-level PSD.

10 Grand average PSD (mean+standard error) for the PD group (blue) and healthy control group (red).

11 Figure 3: Regression analysis of PSD features.

12 Standardized regression coefficients for the analyses of sensorimotor PSD features as a function of
13 group, age, sex, cortical thickness and the interaction between these factors. * indicate factors with
14 Bayes Factor > 3 in the model comparison.

15 Figure 4: Regression analysis of burst features.

16 Standardized regression coefficients for the analyses of burst features as a function of group, age, sex,
17 cortical thickness and the interaction between these factors. * indicate factors with Bayes Factor > 3 in
18 the model comparison.

19 **Figure 5: Age-related changes in sensorimotor signal features.**

20 Scatterplots of the individual measures and model predictions over age for (A) burst rate, (B) PSD
21 broadband 1/f intercept, and (C) PSD broadband 1/f exponent, split between PD patients (blue) and
22 healthy controls (red), and female (solid) and male (dashed).

23 **Figure 6: Regression analysis of motor symptoms.**

24 Standardized regression coefficients for the regression analyses of sensorimotor signal features on
25 clinical motor symptom ratings in PD. * indicate factors with Bayes Factor > 3 in the model
26 comparison.

27 **Tables**

28 **Table 1**

29 Group-level summary of the participants included in the analysis. Mean (standard deviation).

Measure	Parkinson's patients	Healthy controls	Statistics
<i>N</i>	78	60	
<i>Sex (female/male)</i>	29/49	27/33	$\chi^2 = 0.57, p = 0.45$
<i>Age</i>	65.6 (9.5)	63.93 (8.4)	Welsh $t(138.0) = 1.08, p = 0.28$
<i>Disease duration</i>	4.4 (3.7) years	-	-
<i>LEDD</i>	548 (273) mg	-	-
<i>MDS-UPDRS-III</i>	18.9 (10.8)	-	-
<i>MoCA</i>	26.1 (2.8)	26.2 (2.1)	Welsh $t(136) = 0.10, p = 0.92$

30

31 **Table 2**

32 Summary explanations of the main outcome variables in the analysis

Variable category	Variable	Explanation
PSD	<i>Beta power</i>	The maximum peak in the 13-30 Hz band. Estimated as the height of the Gaussian function fitted to the PSD after regressing out the 1/f spectrum.
	<i>Beta centre frequency (Hz)</i>	The dominant frequency bin in the 13-30 Hz band. Estimated as the centre of the Gaussian function fitted to the 13-30 Hz range of the PSD after regressing out the 1/f spectrum.
	<i>Alpha power</i>	The maximum peak in the 8-12 Hz band. Estimated as the height of the Gaussian function fitted to the PSD after regressing out the 1/f spectrum.
	<i>Alpha centre frequency (Hz)</i>	The dominant frequency bin in the 8-12 Hz band. Estimated as the centre of the Gaussian function fitted to the 8-12 Hz range of the PSD after regressing out the 1/f spectrum.
	<i>1/f offset</i>	The intercept of the log-linear regression line estimated from the full PSD in the 0.5-40 Hz range.
	<i>1/f exponent</i>	The decay exponent ($1/f^k$) of the PSD, corresponding to the slope of the log-linear regression line, estimated from the full PSD in the 0.5-40 Hz range.
Burst	<i>Rate</i>	The number of burst events in the time series divided by the length of the time series
	<i>Duration (ms)</i>	The time point from where the signal envelope rise above the threshold until the next time point it drops below the threshold.
	<i>Interval (ms)</i>	The time point from where the signal envelope drops below the threshold until the next time point it rises above the threshold.
	<i>Amplitude</i>	The maximum envelope amplitude within a burst event.

33